Supplement of

Soil moisture-atmosphere coupling strength over Central Europe in the recent warming climate

Thomas Schwitalla et al.

Correspondence to: Thomas Schwitalla (Thomas.Schwitalla@uni-hohenheim.de)

Supplementary Figure S1 displays the ERA5 soil type and its associated field capacity and wilting point.

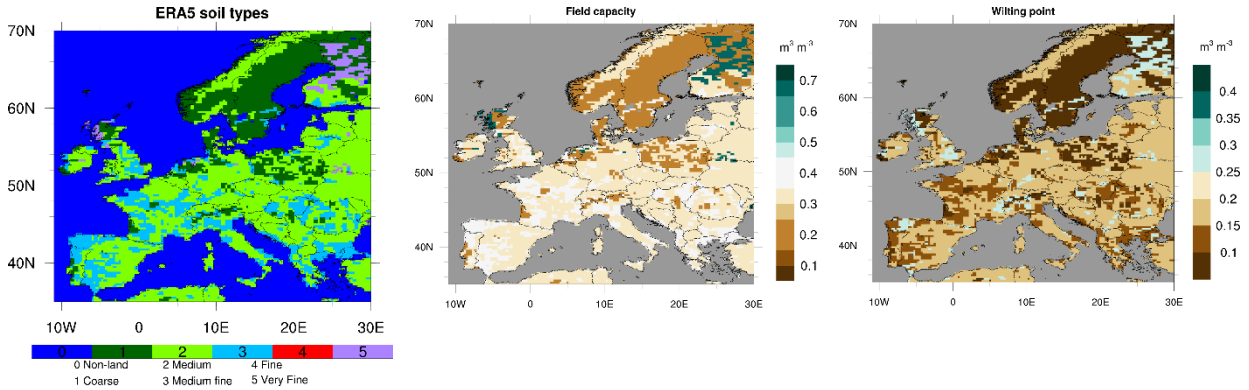

Figure S1. ERA5 soil texture type (left), field capacity (middle) and wilting point (right).

Supplementary figures S2-S5 display the ERA5 500 hPa geopotential, ERA5 2-m temperature, EOBS precipitation, and ERA5 root zone soil moisture anomalies relative to the reference period 1991-2020.

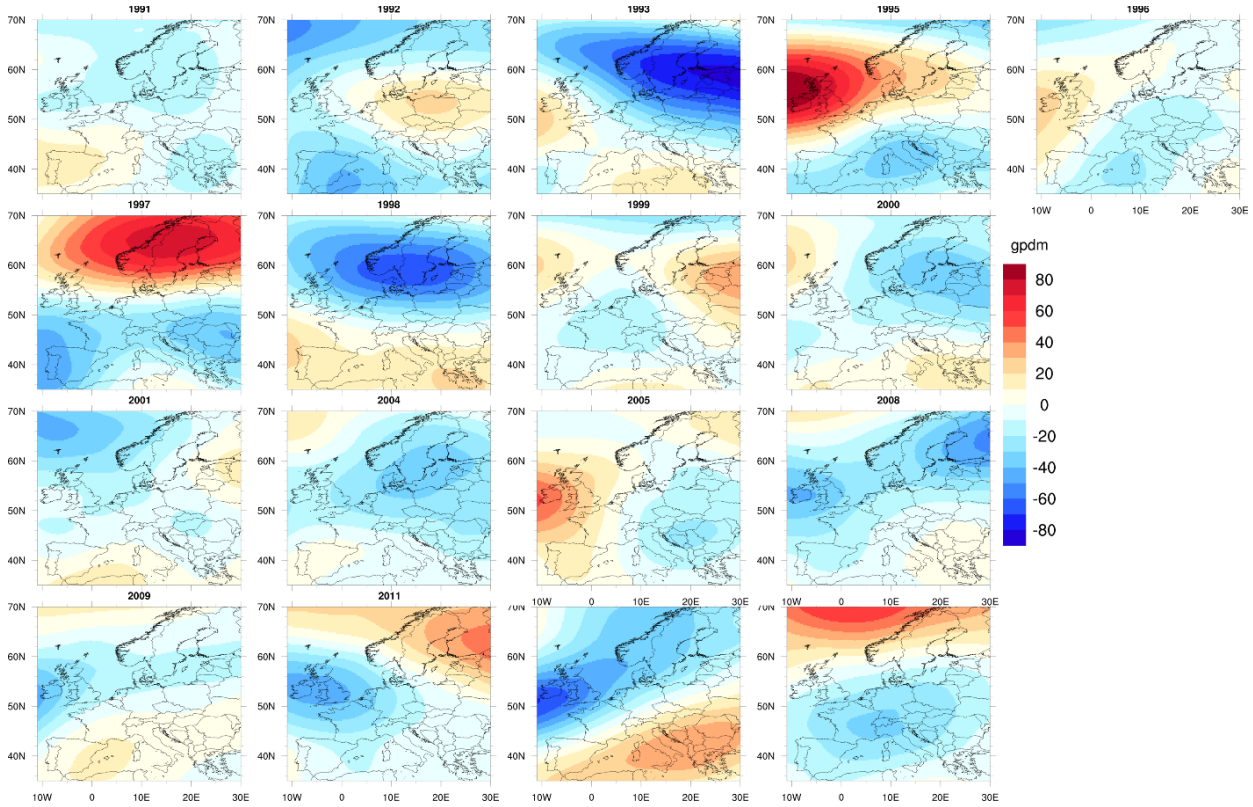

Figure S2. ERA5 500 hPa geopotential anomalies for the cold summer seasons defined in Table 1 relative to the reference period 1991-2020.

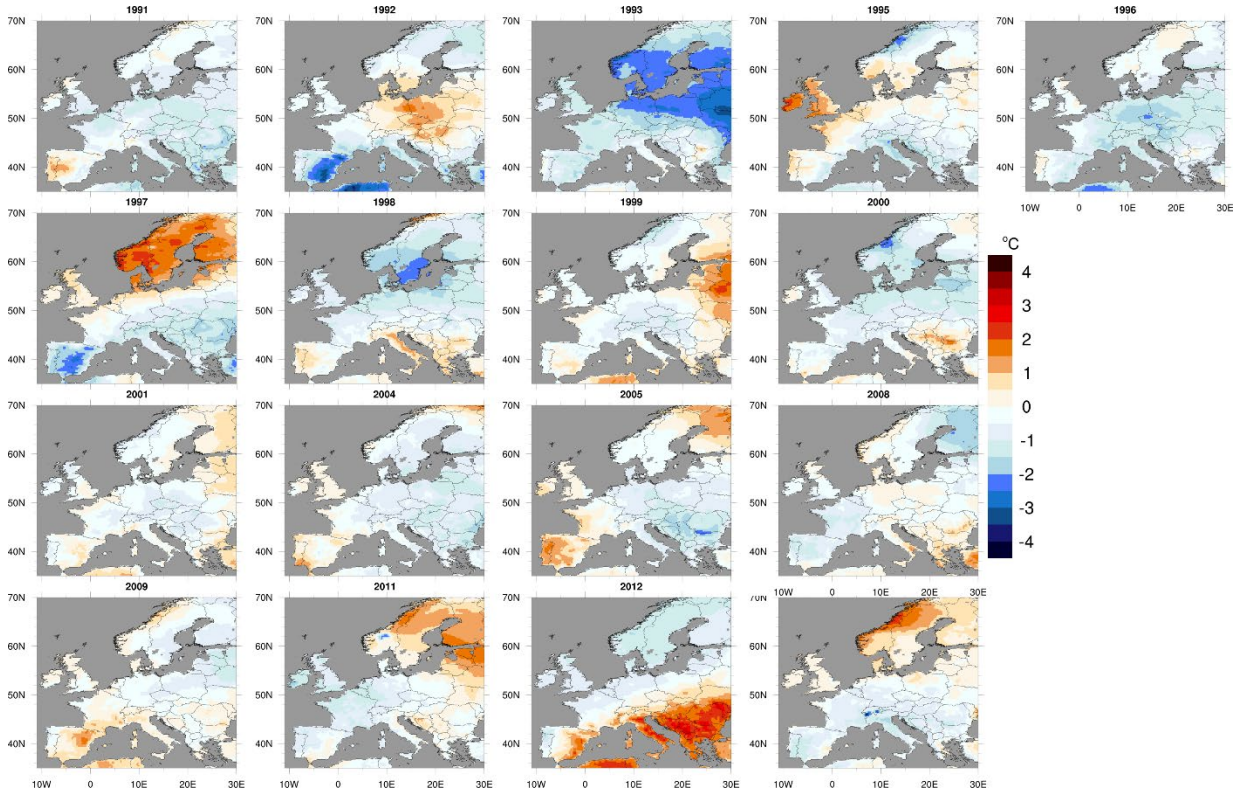

Figure S3. ERA5 2-m temperature anomalies for the cold summer seasons defined in Table 1 relative to the reference period 1991-2020.

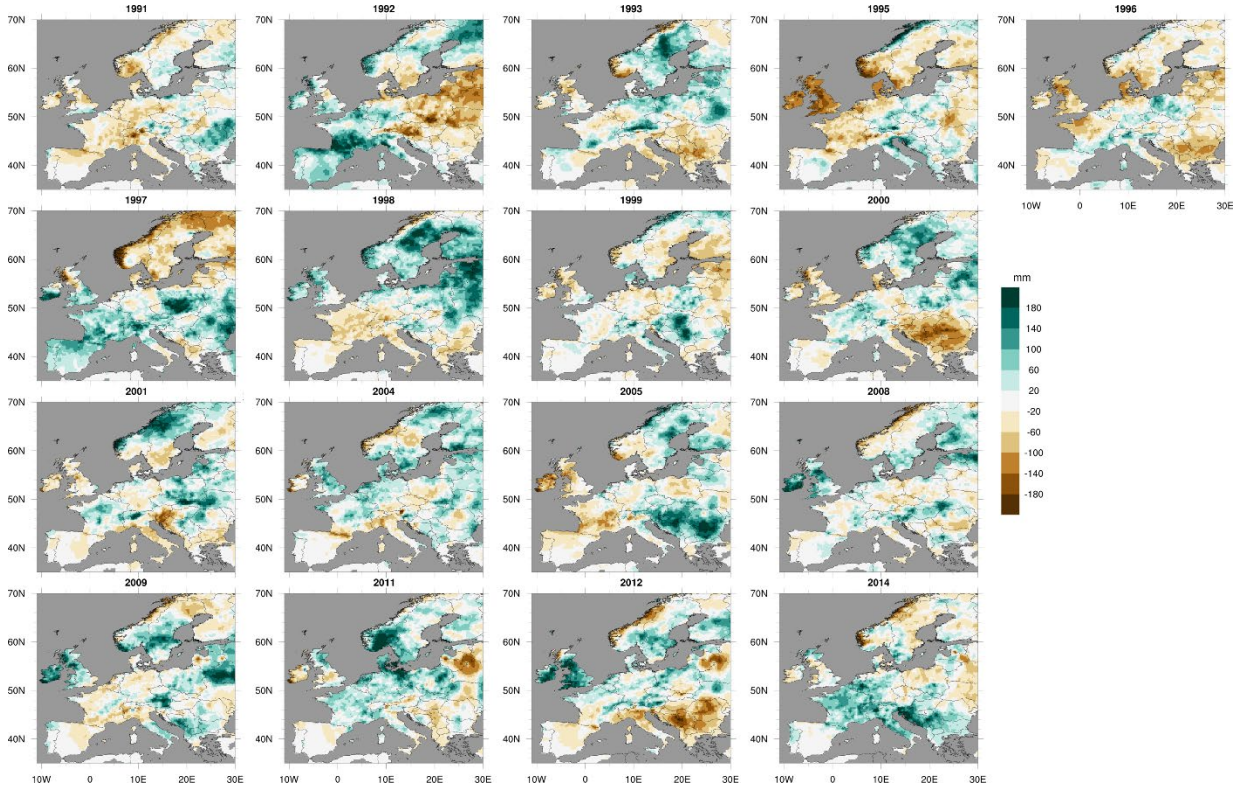

Figure S4. EOBS precipitation anomalies for the cold summer seasons defined in Table 1 relative to the reference period 1991-2020.

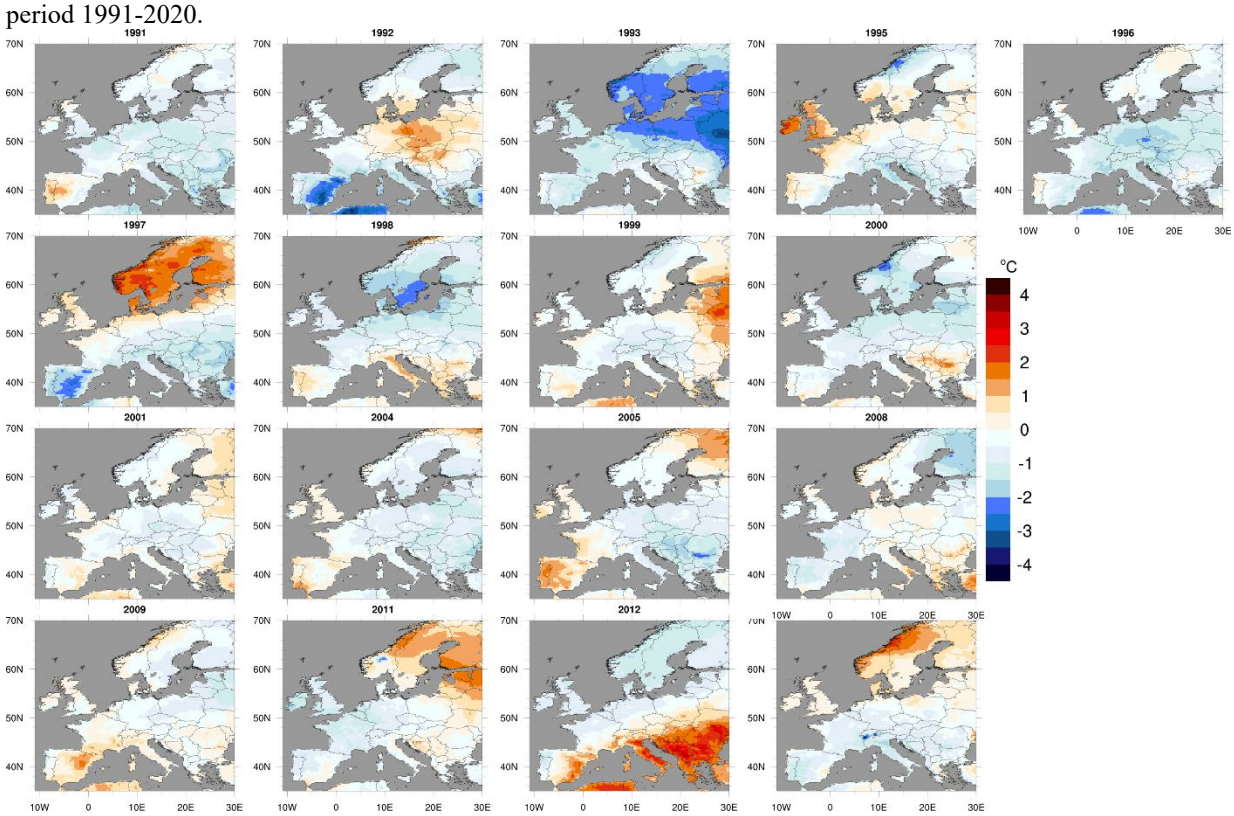

Figure S5. ERA5 root zone soil moisture anomalies for the cold summer seasons defined in Table 1 relative to the reference period 1991-2020.

Supplementary Figure S6 displays the two-legged coupling index (TLCI) between root zone soil moisture, surface latent heat flux (LH) and convective available potential energy (CAPE).

In this case the terrestrial and atmospheric legs are combined in a "two-legged" index (TLCI; Dirmeyer et al., 2014)

$$TLCI = \sigma(\eta)\frac{dLH}{d\eta}\frac{dCAPE}{dLH} \qquad (1)$$

This allows for describing, e.g., the root zone soil moisture impacts CAPE via the surface latent heat flux (Warrach-Sagi et al., 2022).

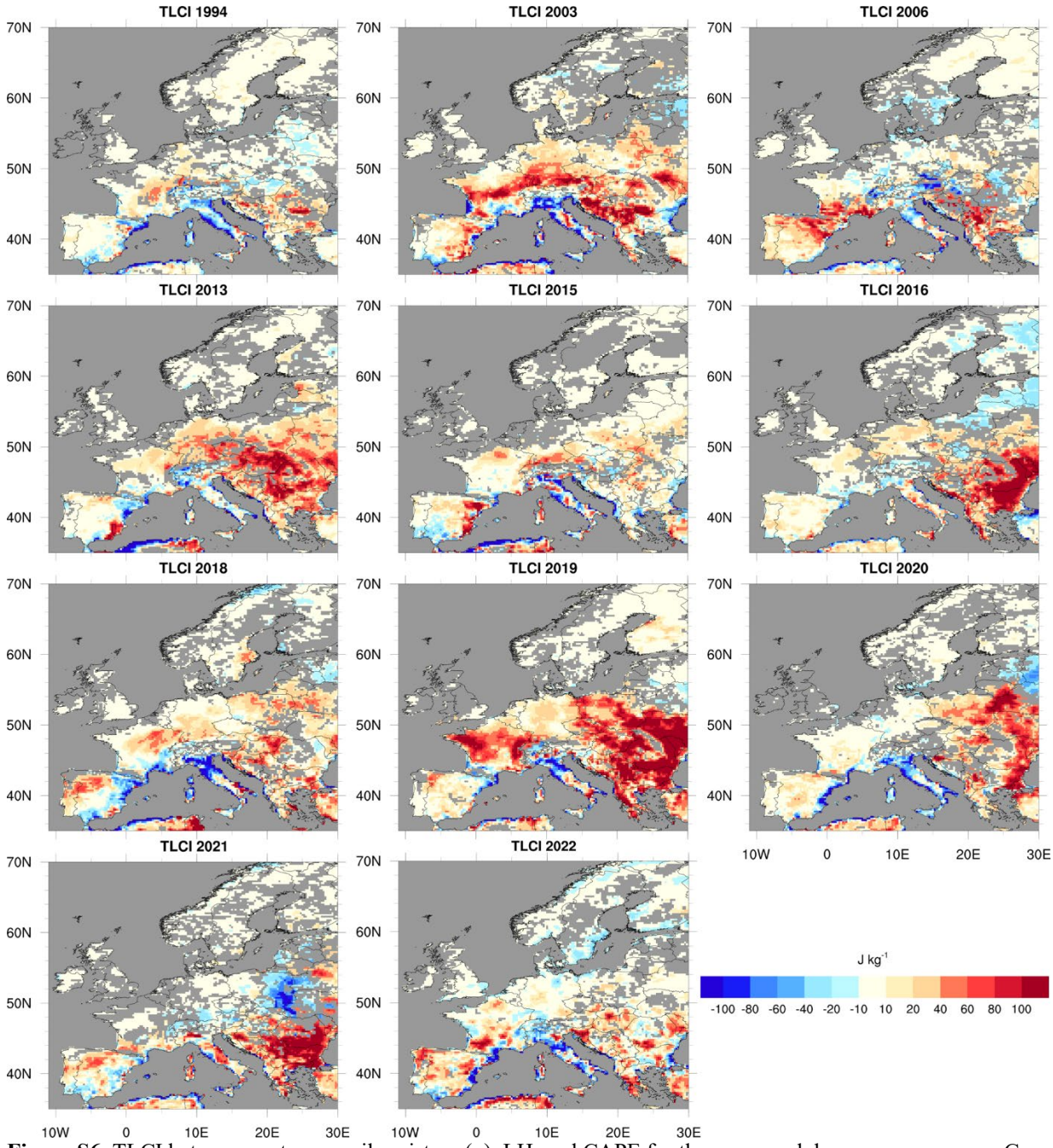

Figure S6. TLCI between root zone soil moisture (η), LH, and CAPE for the warm and dry summer seasons. Grey areas denote water grid cells and statistically non-significant TLCIs over land.

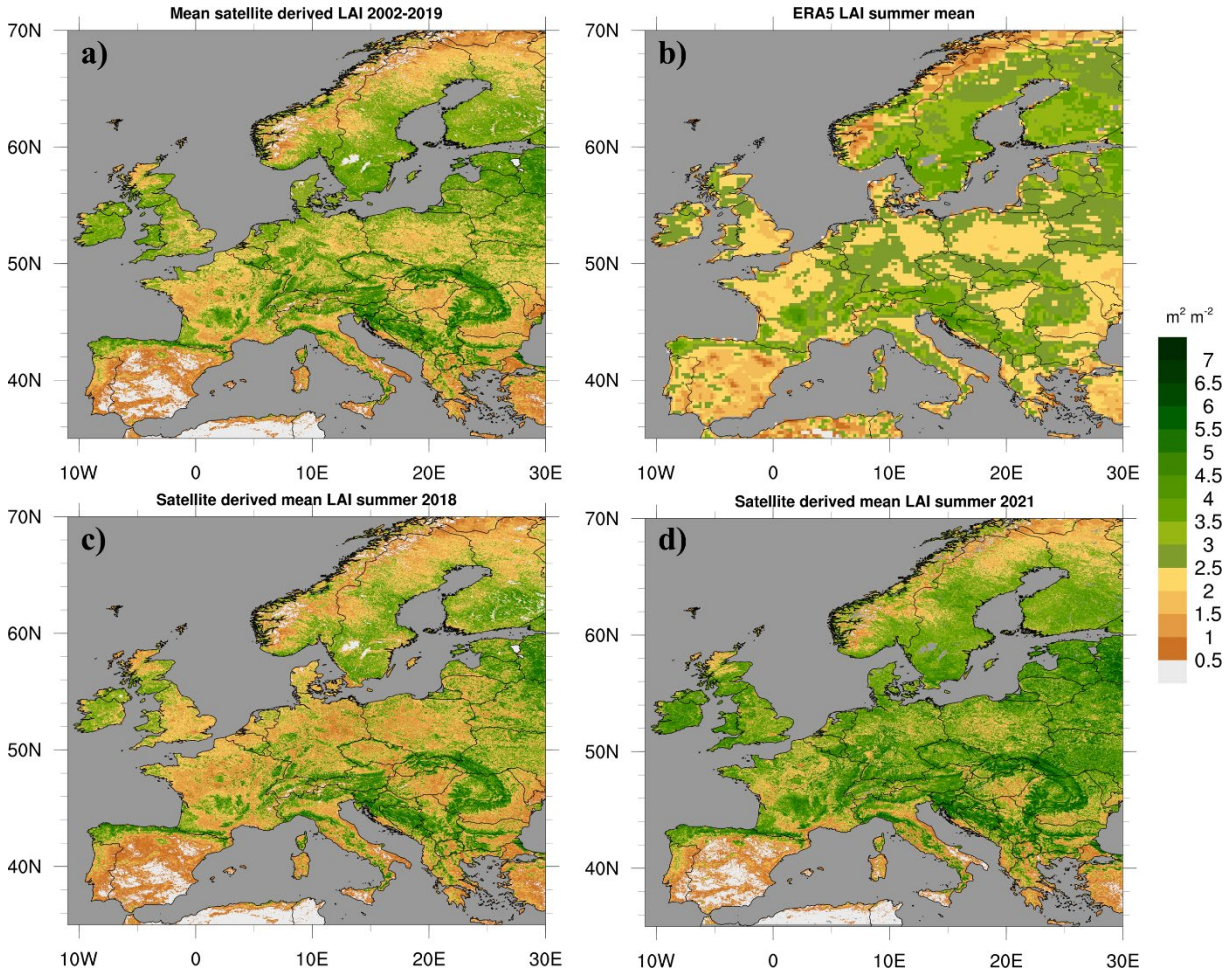

Figure S7. Mean summer LAI for the period 2002-2019 derived from satellite data (a), from ERA5 climatology (b), and derived from satellite data for 2018 (c) and 2021 (d).

References

Dirmeyer, P. A., Wang, Z., Mbuh, M. J., and Norton, H. E.: Intensified land surface control on boundary layer growth in a changing climate, Geophys. Res. Lett., 41, 1290–1294, https://doi.org/10.1002/2013GL058826, 2014.

Warrach-Sagi, K., Ingwersen, J., Schwitalla, T., Troost, C., Aurbacher, J., Jach, L., Berger, T., Streck, T., and Wulfmeyer, V.: Noah-MP With the Generic Crop Growth Model Gecros in the WRF Model: Effects of Dynamic Crop Growth on Land-Atmosphere Interaction, Journal of Geophysical Research: Atmospheres, 127, https://doi.org/10.1029/2022JD036518, 2022.